# Alpha-Particle-Induced Breakup of the Deuteron*

K. NAGATANI,† T. A. TOMBRELLO,‡ AND D. A. BROMLEY
*Yale University, New Haven, Connecticut*
(Received 13 July 1965)

Alpha-particle-induced deuteron breakup reactions have been studied in single-counter measurements at incident alpha-particle energies of 41.6 and 29.3 MeV. Simultaneous differential and total cross-section measurements have been carried out on protons, deuterons, and alpha particles. Unambiguous evidence for final-state resonance effects in the alpha-nucleon interactions have been obtained, particularly from the proton energy spectra; the $p_{3/2}$ alpha-nucleon resonances corresponding to the $He^5$ and $Li^5$ ground states play important roles. As anticipated, phase-space-factor and zero-range Born-approximation calculations failed to reproduce the observed energy spectra. A more exact analysis which explicitly includes the alpha-nucleon interactions, represented by Gammel-Thaler phenomenological potentials, does provide good agreement with the experimental results both in spectrum shape and in total breakup cross section.

## INTRODUCTION

UNTIL very recently, nuclear-reaction studies have been almost entirely restricted to binary-exit-channel systems. With increasing understanding of nuclear-reaction mechanisms and, in particular, more sophisticated instrumentation, interest has been focused on the more complex situations which characterize multibody-reaction exit channels. Of particular interest in these reactions is the possibility of observing phenomena attributable to the presence of short-lived nuclear complexes involving two or more of the reaction participants in the exit channel. These phenomena have come to be known as "final-state interactions" and will be so characterized herein; it should be emphasized that this does not imply the more restricted definition first used by Watson[1] at higher energies.

Of the interactions leading to three-body final channels, those involving breakup of the deuteron have been most readily accessible and most thoroughly studied to date. Deuteron breakup induced by nucleons has received the most extensive study, both experimental[2–10] and theoretical.[11–16] As yet no entirely satisfactory theoretical analysis of these experimental data has been recorded.

It may be argued that one of the simplest three-body cases is that following alpha-particle-induced breakup of the deuteron because below the alpha-particle breakup threshold only one inelastic channel is open, namely, that corresponding to $\alpha+d\rightarrow\alpha+p+n$. A number of experimental studies[3,8,17–21] have already been reported on this particular breakup reaction; however, here again the measurements have been somewhat limited in their scope. Measurements have been reported at single incident energies or for only a restricted range of angles.

Of particular interest in this case are the alpha-particle-nucleon interactions to the extent that they condition the characteristics of the exit channel; below the alpha-particle breakup threshold, the alpha particle may be regarded as a single entity and the neutron-proton interaction in the final state is expected to influence the situation only through its continuum scattering state rather than its virtual state, which, in the particular reaction chosen, is isotopic-spin forbidden. Rybakov *et al.*[18] have reported a theoretical analysis of the available experimental data; however, as pointed out by Lefevre *et al.*,[20] the analysis is ambiguous in several respects and does not represent a satisfactory treatment of the data.

The work to be reported herein was carried out in an attempt, first, to provide a comprehensive set of experi-

* Supported by U. S. Atomic Energy Commission.
† Present address: Laboratory for Nuclear Science, Massachusetts Institute of Technology, Cambridge, Massachusetts.
‡ Present address: Kellogg Radiation Laboratory, California Institute of Technology, Pasadena, California.

1 K. M. Watson, Phys. Rev. **88**, 1163 (1952).
2 W. H. Barks and P. B. Treacy, Phys. Rev. **56**, 288 (1939).
3 R. L. Hankel, J. E. Perry, Jr., and R. K. Smith, Phys. Rev. **99**, 1050 (1955).
4 M. P. Nakada, J. D. Anderson, C. C. Gardner, J. McClure, and C. Wang, Phys. Rev. **110**, 594 (1958).
5 A. T. G. Furguson and G. C. Morrison, Nucl. Phys. **5**, 41 (1958).
6 L. Cranberg and R. K. Smith, Phys. Rev. **113**, 587 (1959).
7 C. Wang, J. D. Anderson, C. C. Gardner, J. W. McClure, and M. P. Nakada, Phys. Rev. **116**, 164 (1959).
8 B. V. Rybakov, V. A. Sidrov, and N. A. Vlasov, Nucl. Phys. **23**, 491 (1961).
9 K. Ilakovac, L. G. Kuo, M. Petravić, I. Šlaus, and P. Tomaš, Phys. Rev. Letters **6**, 356 (1961).
10 P. F. Donovan, Rev. Mod. Phys. **37**, (1965); P. F. Donovan, J. V. Kane, J. F. Mollenauer, and Č. Zupančič, *Proceedings International Congress on Nuclear Physics, Paris* (Paris, 1964), Vol. 2, p. 238.
11 Č. Zupančič, Rev. Mod. Phys. **37**, 330 (1965).
12 R. M. Frank and J. L. Gammel, Phys. Rev. **93**, 463 (1954).
13 W. Heckrotte and M. MacGregor, Phys. Rev. **111**, 593 (1958).
14 L. Castillejo and L. S. Singh, *Nuclear Forces and the Few-Nucleon Problems*, edited by T. C. Griffith and E. A. Power, (Pergamon Press, Inc., London, 1960), Vol. 1, p. 193.
15 K. Ilakovac, L. G. Kuo, M. Petravić, I. Šlaus, and P. Tomaš, Nucl. Phys. **43**, 254 (1963).
16 R. J. N. Phillips, Nucl. Phys. **53**, 650 (1964).
17 J. C. Allred, D. K. Froman, A. M. Hudson, and L. Rosen, Phys. Rev. **82**, 786 (1951).
18 E. W. Warburton and J. N. McGruer, Phys. Rev. **105**, 639 (1957).
19 K. P. Artemov and N. A. Vlasov, Zh. Eksperim. i Teor. Fiz. **39**, 1612 (1960) [English transl.: Soviet Phys.—JETP **12**, 1124 (1961)].
20 H. W. Lefevre, R. R. Borchers and C. H. Poppe, Phys. Rev. **128**, 1328 (1962).
21 P. F. Donovan and J. F. Mollenauer (private communication).

mental data on the alpha-induced deuteron breakup reaction and, second, to carry out a somewhat more systematic examination of the possible analyses of these data to highlight the final-state interactions present.

Experimental studies have been carried out on both product alpha particles and protons over a wide range of observation angles and with incident-alpha-particle energies of both 41.6 and 29.3 MeV. At the same time, the elastic deuteron energy spectra and angular distributions have been obtained for use in normalization of the breakup cross sections and for comparison with previous scattering results at slightly different energies. In order to disentangle the complex kinematic situation which represents the multibody reaction channel, it is highly desirable to carry out particle-particle coincidence studies involving selected reaction products. These were unfortunately precluded, in the present work, by the duty cycle of the linear accelerator used to provide the alpha-particle beam. In consequence, the data to be presented were all noncoincident and were obtained with single counters or with counter telescopes where appropriate. This has the unfortunate consequence of greatly complicating any theoretical analysis in requiring integration over all unobserved coordinates; on the other hand, it does provide an over-all survey of the reaction characteristics which is not obtained except in a most complete coincidence study.

Clear evidence for the importance of the $p_{3/2}$ resonance in the alpha-neutron interaction, corresponding to the $He^5$ ground state, has been found in the energy spectra of product protons from the breakup reaction. The corresponding resonance in the alpha-proton interaction, corresponding to the $Li^5$ ground state, has been found to play a similar role although under the conditions of the present experiments its effect is not as striking as that of the alpha-neutron resonance. Absolute cross sections were determined both directly from measurement of the detection efficiencies and integration of the incident beam and from comparison with previously measured precise elastic-scattering cross sections for deuterons on helium.

It was found that the alpha-particle spectra were essentially featureless and not readily amenable to analysis; relatively detailed analyses, however, have been carried out on the proton spectra which showed pronounced structure.

Purely for orientation purposes the experimental spectra were compared with the simple predictions based on phase-space considerations, although it was recognized that these could not reproduce any structure in the spectra. A zero-range Born-approximation calculation has been shown[11] to have some relevance to the results obtained in nucleon-induced deuteron breakup; moreover, it has provided a convenient framework for the discussion of a number of the particle-particle coincidence studies on a few nucleon systems carried out by the Brookhaven group.[10,11,21] In particular, these zero-range Born approximation calculations made obvious the identification of spectator-pole behavior, wherein one of the nucleons in the target deuteron functions only as a spectator in the breakup.

It would not be anticipated that such phenomena would have marked effects on the integrated spectra measured here; however, it was considered of interest to carry through these calculations appropriate to the present data.

As anticipated, the phase-space or the Born-approximation calculations did not predict spectra having the structural characteristics of those observed. It should again be emphasized that the present measurements would be extremely insensitive to these amplitudes.

Finally, a more complete calculation was performed in which the alpha-nucleon resonances, which kinematic arguments suggested were responsible for the spectrum structure, were included explicitly through use of the phenomenological Gammel-Thaler potentials. In view of the complexity of these latter calculations, they have been completed for only a single angle of observation (12.6°) and at that angle have achieved an adequate representation of both the experimental spectrum and of the absolute cross section. As carried through, the calculations included a number of approximations which will be discussed below; in view of the success attained at 12.6°, however, the calculations are being refined and the results of these together with the details of the calculations themselves will be presented in a later paper.

## II. EXPERIMENTAL PROCEDURES

### A. Beam Handling and Target

The alpha-particle beam from the Yale Heavy Ion Linear Accelerator has been utilized in the studies to be reported here. The direct beam from the accelerator has an energy, following magnetic analysis, of 42.1 MeV; the lower energy of 29.8 MeV was achieved by inserting absorber foils in the beam prior to magnetic analysis. In both cases, the final energies on target are known from the calibration of the analysis system to an accuracy of better than 0.6%.

The collimated beam from the accelerator was incident upon a gas target cell having windows of 0.00013-in. Havar foil for both incident and transmitted beam and was collected and integrated in a Faraday cage assembly. The window geometry permitted detection of reaction products at all angles with respect to the incident beam. The purity of the deuterium gas used in the target was examined by mass spectroscopy where it was found that the only significant impurity was $H_2$ at less than 0.3%; this finding was confirmed by the observation of the elastically scattered recoil-proton peaks in the experimental spectra. All other target contaminants were found to be present in negligible proportion.

During the experimental measurements the deuterium pressure was maintained constant to considerably better than 1%, using a standard Cartesian manostat, at selected values between 20 and 30 in. of mercury, absolute. The gas temperature was monitored during all measurements using a thermometer system in direct thermal contact with the target cell. Only very small temperature variations were observed and cross-section data have been appropriately corrected for them. Under measurement conditions the incident alpha-particle beam at 42.1 MeV lost 0.48 MeV in reaching the target center through the entrance window and the target gas.

### B. Detection System

A standard semiconductor $dE/dx \times E$ counter telescope was assembled in order to identify and separate the different charged-particle species resulting from the interaction. The transmission counter was an ORTEC Au-Si surface barrier detector with a 59-$\mu$ depletion thickness; the residual energy detector was a lithium-drifted silicon unit fabricated in this laboratory[22] with approximately 5-mm active thickness. Since at backward angles only low-energy protons were permitted, because of kinematic considerations, the counter telescope was unnecessary and a single semiconductor detector having 170-$\mu$ depletion thickness was used at these angles.

The energy resolution of the residual energy detector was 250 keV for 5.5-MeV alpha particles and was 30 keV for each of the transmission detectors. The detector systems were mounted on a movable lid on the scattering chamber permitting continuous variation of observation angles. Extensive collimation was provided, including antiscattering baffles, in order to define precisely the effective target volume utilized in the gas target. The angular aperture of the collimation system used with the counter telescope was $\pm 1.0°$, and with the angle counter used at back angles, $\pm 1.8°$. The solid angles for the various collimator systems were calculated using Silverstein's formulation.[23]

A second 5-mm-thick lithium-drifted silicon detector was used in all measurements as a fixed angle monitor. In order to minimize noise contributions from the detectors a refrigeration system was used to maintain all of them at 10°C. This temperature was chosen as adequate while minimizing condensation problems.

Standard transistorized nuclear instrumentation has been used throughout and the detector signals following amplification have been registered on a Victoreen multiparameter analyzer operated in a $200 \times 100 \times 10^6$ memory configuration. Apart from very low-energy background in the transmission detector, reflecting the presence of gamma radiation and neutrons, the only charged particles registered by the system were alpha particles, deuterons, and protons. The separation achieved by the counter telescope was more than adequate to permit completely unambiguous separation and study of the three species.

### C. Calibrations

The system was calibrated by examining the scattering of the incident alpha particles from hydrogen and helium gas targets. It was found that the energy linearity of the system was better than $\pm 3\%$ after correcting for obvious energy losses. The over-all proton energy resolution was measured in the study of the $\alpha + p$ scattering and was found to be 0.55, 0.98, and 1.00 MeV, respectively, at proton energies of 25.0, 15.0, and 4.0 MeV, respectively. This resolution width is almost entirely due to the kinematic variation of the proton energy with angle and the finite detector apertures used.

The $\alpha + p$ scattering measurements were also used to establish a standard detector response to a monoenergetic proton group. It was found that this could be represented by a Gaussian peak and a low-energy tail of constant amplitude extending downward from the peak energy. In order to obtain a realistic proton energy spectrum, particularly in a case such as the present one where a large continuous contribution is anticipated, it is essential that this low-energy tail, although negligibly small in the case of an individual proton group, be taken into account. The tail is probably due

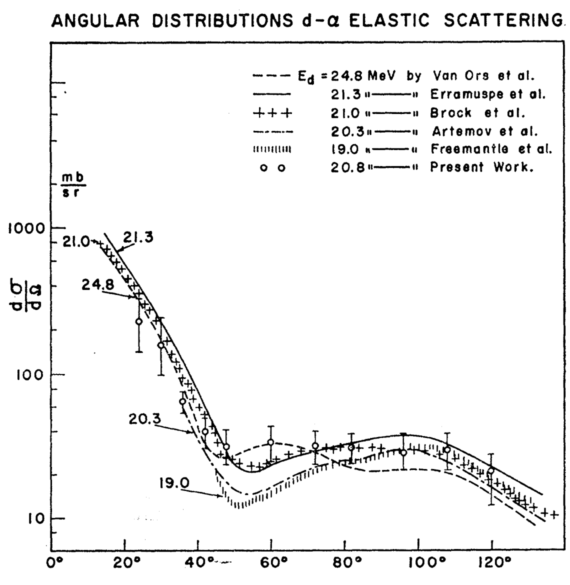


FIG. 1. Compilation of angular distributions from alpha particle plus deuteron elastic scattering. The quoted energies are in the center-of-mass system and are used to label the different experimental results.

[22] C. Chasman and J. Allen, Nucl. Instr. Methods 24, 253 (1963).
[23] E. A. Silverstein, Nucl. Instr. Methods 4, 53 (1959).

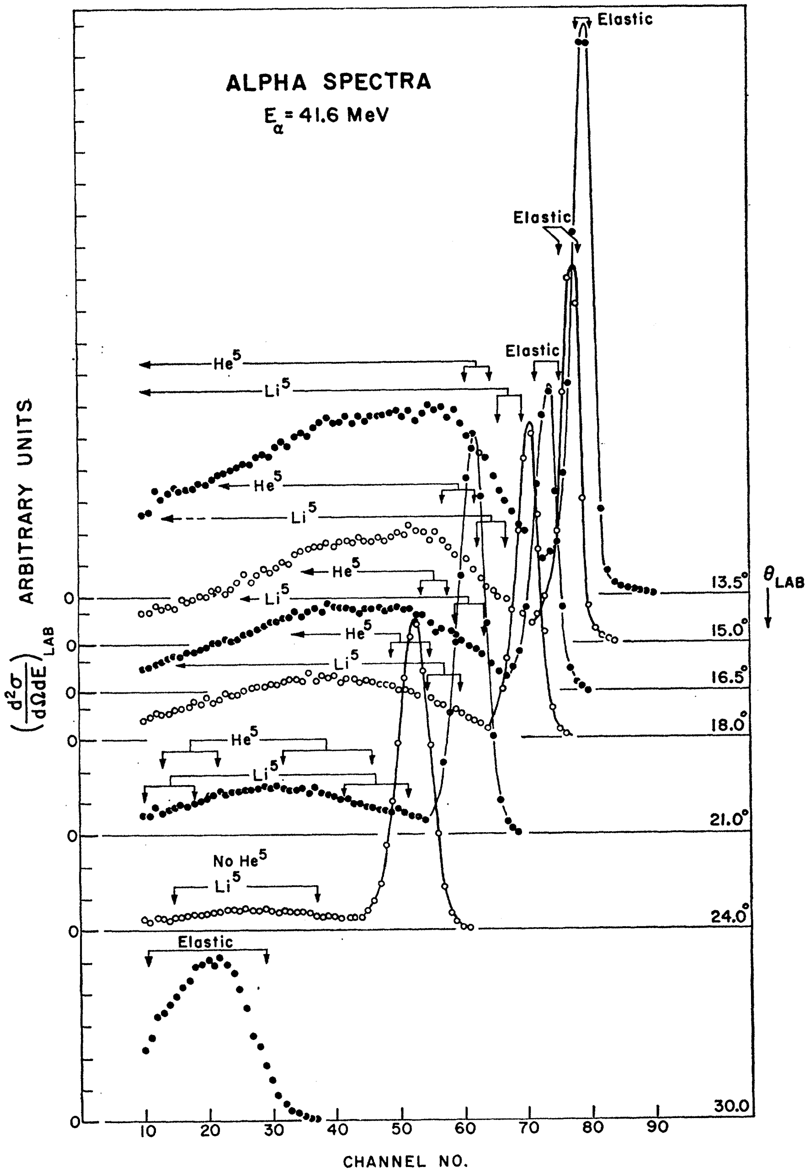


FIG. 2. Alpha-particle energy spectra from deuteron dissociation reactions induced by 41.6-MeV alpha particles. Laboratory energies are shown in terms of channel numbers and the differential cross sections have been arbitrarily normalized for display presentation. Kinematic predictions for various processes together with associated kinematic broadenings are indicated by the superposed arrows as discussed in the text.

to multiple scattering in the gas cell (both foils and gas) and from the slit edges of the beam and detector collimators.

The particular energy spectrum taken at 12.6°, which will be compared with the theoretical analysis to be presented herein has been corrected for this detector response as will be indicated in later figures. Because an exact matrix inversion which is required to carry out a precise channel-by-channel correction of a spectrum of the present dimensions would be unduly tedious and unnecessary, a number of approximations have been introduced. These approximations together with the uncertainties in the actual experimental tail in the detector response are reflected in an over-all uncertainty in the magnitude of the correction to be applied to the observed spectrum. This too will be indicated in later figures but it is clear that it certainly does not mask, in any significant way, the features of interest in the spectrum. It should be emphasized that the uncertainty obtained is in each case, a maximal one with the anticipated proper result falling midway within the band shown. Equivalent correction has not been carried out on the remaining spectra shown herein.

The absolute reaction cross sections were determined both from measurement of the beam intensities and the system geometry and from comparison of the measured $(\alpha+d)$ elastic scattering with previous precision measurements of that cross section.[24] It was not found possible to obtain a value for this cross section to an accuracy of better than 35%; by far the largest contribution to this uncertainty comes from the instability of

[24] W. T. H. Van Oers and W. K. Brockman, Jr., Nucl. Phys. **44**, 546 (1963).

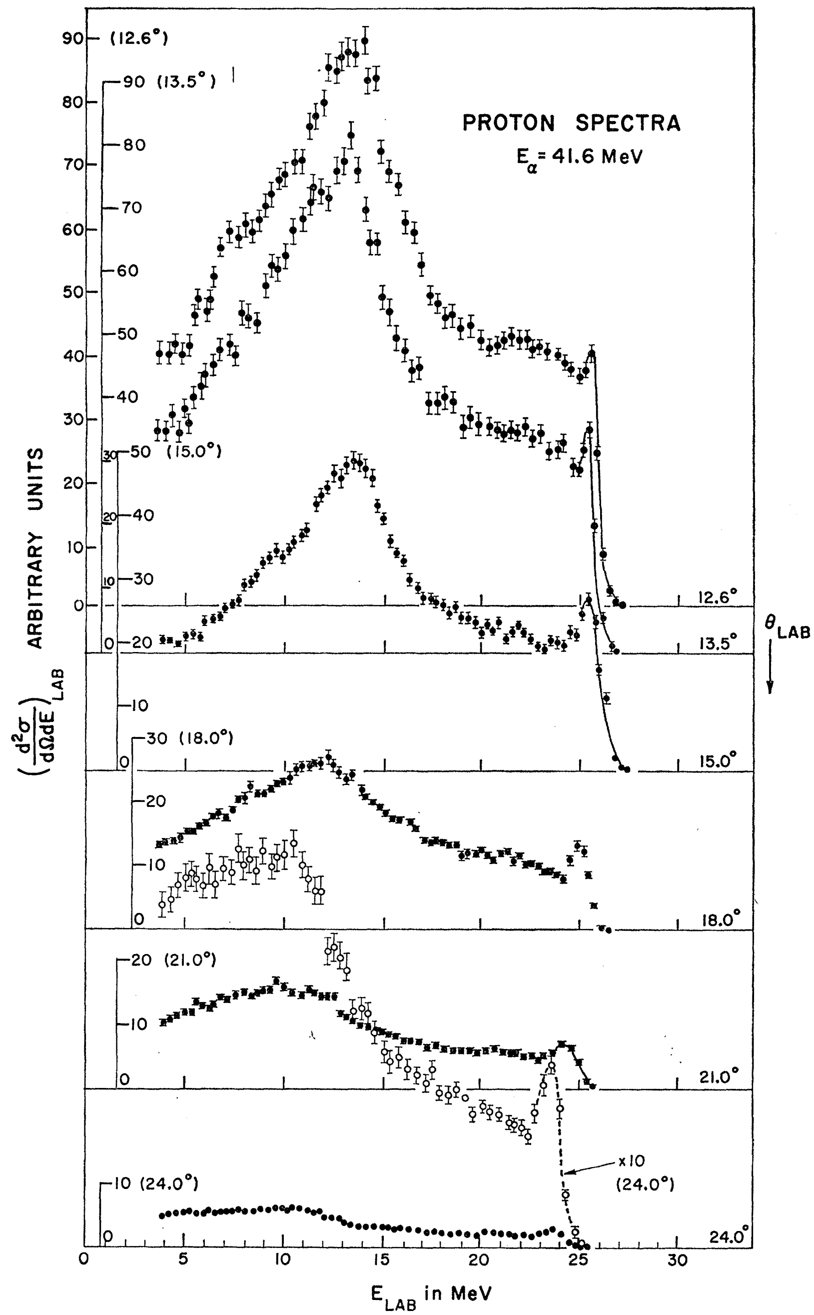


FIG. 3. Proton energy spectra from deuteron breakup reactions induced by alpha particles of 41.6 MeV. The differential cross sections have been arbitrarily normalized. Error bars include statistical errors only, and no correction has been made for the detector response.

the beam optics in the linear accelerator and the consequent variability of the effective target volume utilized in the scattering chamber. Figure 1 compares the angular distribution of elastically scattered deuterons, as measured in the present experiment, with those obtained at slightly different energies in earlier studies[24–27]; as is evident from Fig. 1 the internal agreement is well within the indicated errors.

[25] H. E. Conzett, G. Igo, H. C. Shaw, and R. J. Slobodrian, Phys. Rev. 117, 1075 (1960).

[26] R. G. Freemantle, T. Grotdal, W. M. Gibson, R. McKeague, D. J. Prowse, and J. Rotblat, Phil. Mag. 45, 1090 (1954).

[27] H. W. Broek and J. L. Yntema, Phys. Rev. 135, B678 (1964).

## III. EXPERIMENTAL RESULTS

### A. Alpha-Particle Spectra

Alpha-particle energy spectra, at an incident alpha-particle energy of 41.6 MeV, were obtained at a number of observation angles in the range from 13.5° to 30.0° in the laboratory system; Fig. 2 shows typical spectra thus obtained. The elastic peaks were readily identified from their kinematic behavior. In view of the three-body nature of the reaction, continuous inelastic-energy spectra, as indicated in Fig. 2, are anticipated. However, to the extent that the dissociation reaction is assumed

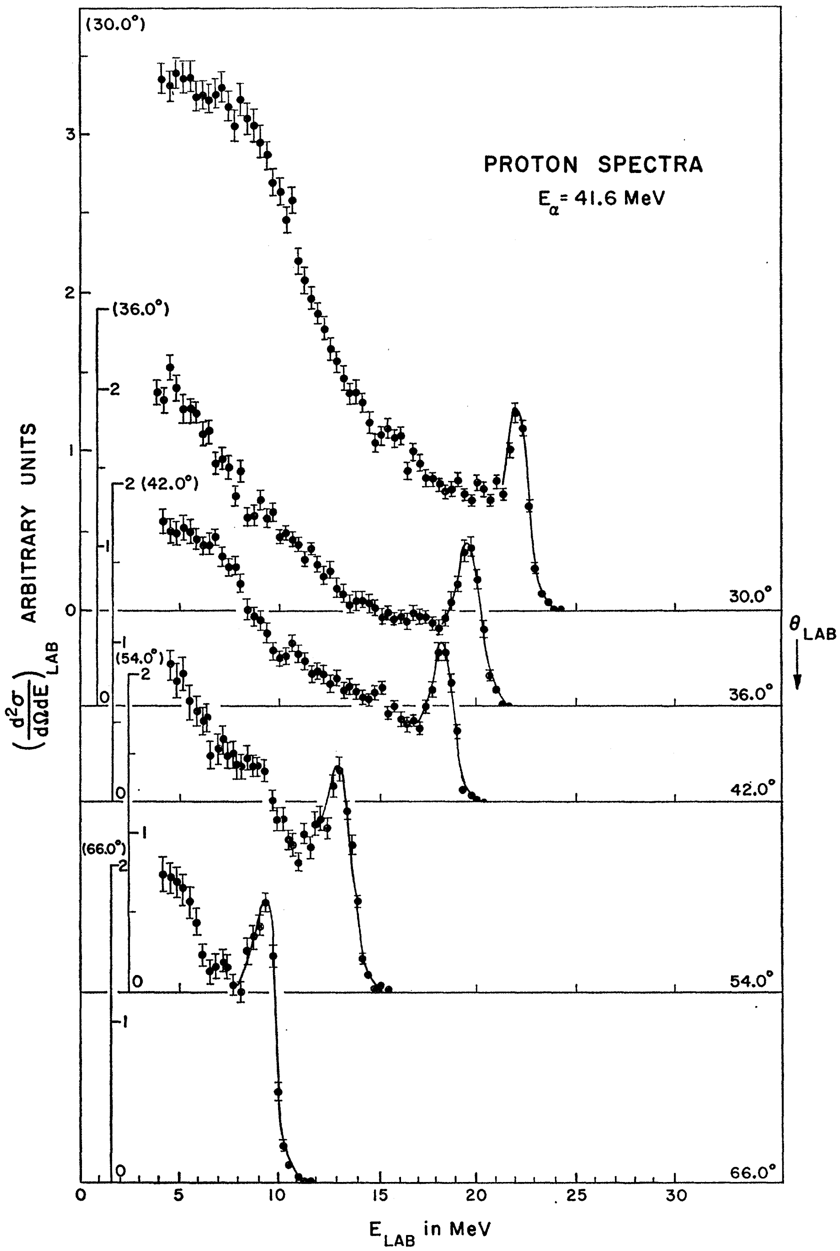


FIG. 4. Proton spectra at larger angles of observation than is Fig. 3.

to proceed sequentially through intermediate states such as

$$\alpha+d\rightarrow \mathrm{He}^5+p\rightarrow \alpha+n+p \tag{1}$$

$$\rightarrow \mathrm{Li}^5+n\rightarrow \alpha+p+n \tag{2}$$

at any given angle of observation the range of alpha-particle energies corresponding to a given process may be calculated. A number of these energy ranges are indicated in Fig. 2. The double arrows in each case indicate the extent of the expected kinematic energy spread because of the finite detector apertures. The purely statistical errors in the spectra are less than 3% in all regions of interest. A search was made for alpha particles beyond the kinematic cutoff at 30° and as, anticipated, none were found.

While these spectra are in good agreement with the results which might be expected on kinematic and open-reaction channel ground, their complexity precludes extraction of any specific information regarding the reaction mechanism.

Equivalent measurements were carried out at an incident alpha-particle energy of 29.3 MeV; it was found that, apart from obvious kinematic shifts, these spectra were identical to those shown in Fig. 2.

### B. Proton Spectra

Figures 3, 4, and 5 present the observed proton spectra measured at an incident alpha-particle energy of 41.6 MeV; Fig. 6 shows those obtained at the reduced incident energy of 29.3 MeV. The indicated errors in these figures are purely statistical.

In each spectrum the energy of the prominent peak at the high-energy end was found to coincide precisely with that expected from the two-body sequential process (1) involving a $He^5$ intermediate state. It should also be noted that the broad maxima, occurring at intermediate energies in the spectra, correspond to the energy range which would be populated by the two-body sequential process (2) involving a $Li^5$ intermediate state. These spectra thus provide convincing evidence for the importance of the $p_{3/2}$ alpha-nucleon resonances in the breakup mechanism under consideration. It should be noted that the spectra taken at the reduced incident energy (Fig. 6) show essentially the same features as those taken at 41.6 MeV. Figure 7 presents an angular distribution for the product protons; in obtaining this angular distribution, the individual spectra have been integrated from an energy of 3.5 MeV to the maximum in the spectrum.

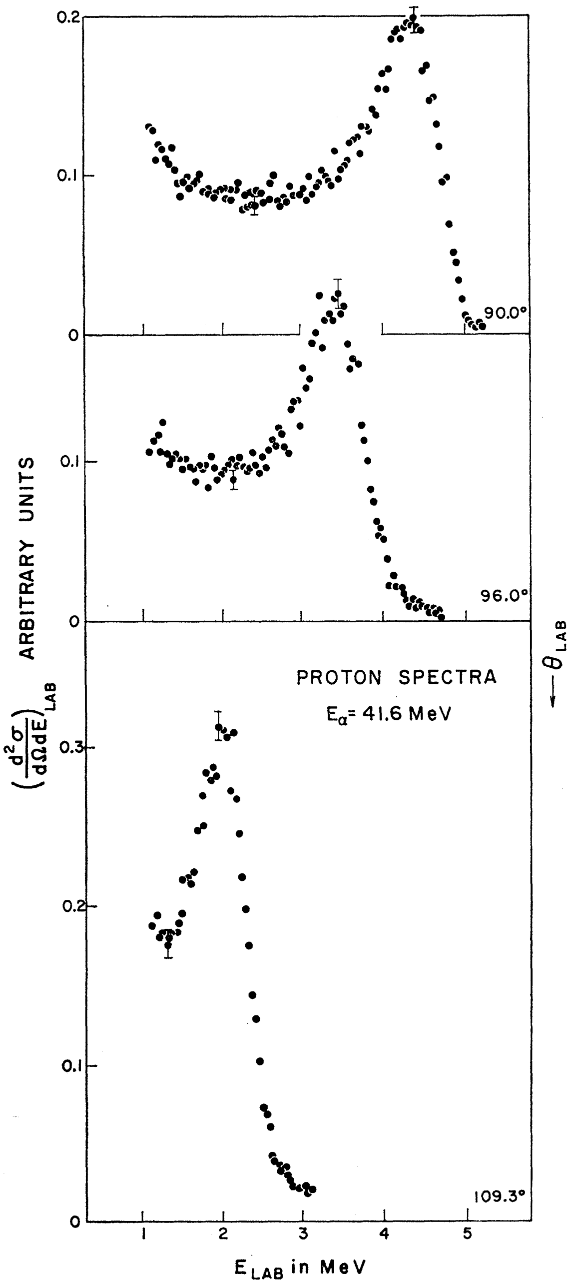


FIG. 5. Proton spectra at larger angles of observation than in Figs. 3 or 4. Here only a single counter rather than a counter telescope was required.

## IV. THEORETICAL ANALYSIS AND DISCUSSION

Figures 8 and 9 present kinematic diagrams appropriate to the present measurements. The only quantitative experimental information obtainable in noncoincident single-particle measurements which may be compared directly with these diagrams is the maximum reaction product energy at a given observation angle. Both the alpha-particle and proton spectra shown in Figs. 2–6 show maximum energies in excellent accord with the kinematic predictions. This is a useful datum since it justifies the implicit assumption which has been made throughout this paper, that the alpha particle remains a bound entity throughout the dissociation reaction.

In general the cross section for the reaction may be written, in terms of the reaction matrix element $M$, as follows:

$$d\sigma=\frac{1}{v_{\text{incident}}}\frac{1}{(2\pi\hbar)^5}\int |M|^2\delta(E_{\text{total}}-E_\alpha-E_p-E_n)$$
$$\times\delta^3(\mathbf{p}_{\text{total}}-\mathbf{p}_\alpha-\mathbf{p}_p-\mathbf{p}_n)d\mathbf{p}_\alpha d\mathbf{p}_p d\mathbf{p}_n. \quad (3)$$

The delta functions appearing in the integrand simply require conservation of energy and of linear momentum and delimit the range of integrations which must be carried out to produce noncoincident spectrum predictions. The various analyses referred to in the Introduction follow from specific choices of the form of the reaction matrix element $M$.

The crudest possible approximation obviously corresponds to constant $M$, resulting in the familiar Fermi phase-space prediction of the multibody reaction spectrum. The rather tedious integrations have been carried out here and elsewhere using the Yale 7040-7094 computer facility and the results of the various approximations are compared with the experimental results in Fig. 10. Curve 1 is the experimental result while curve 2 is the phase-space prediction. The familiar semicircular

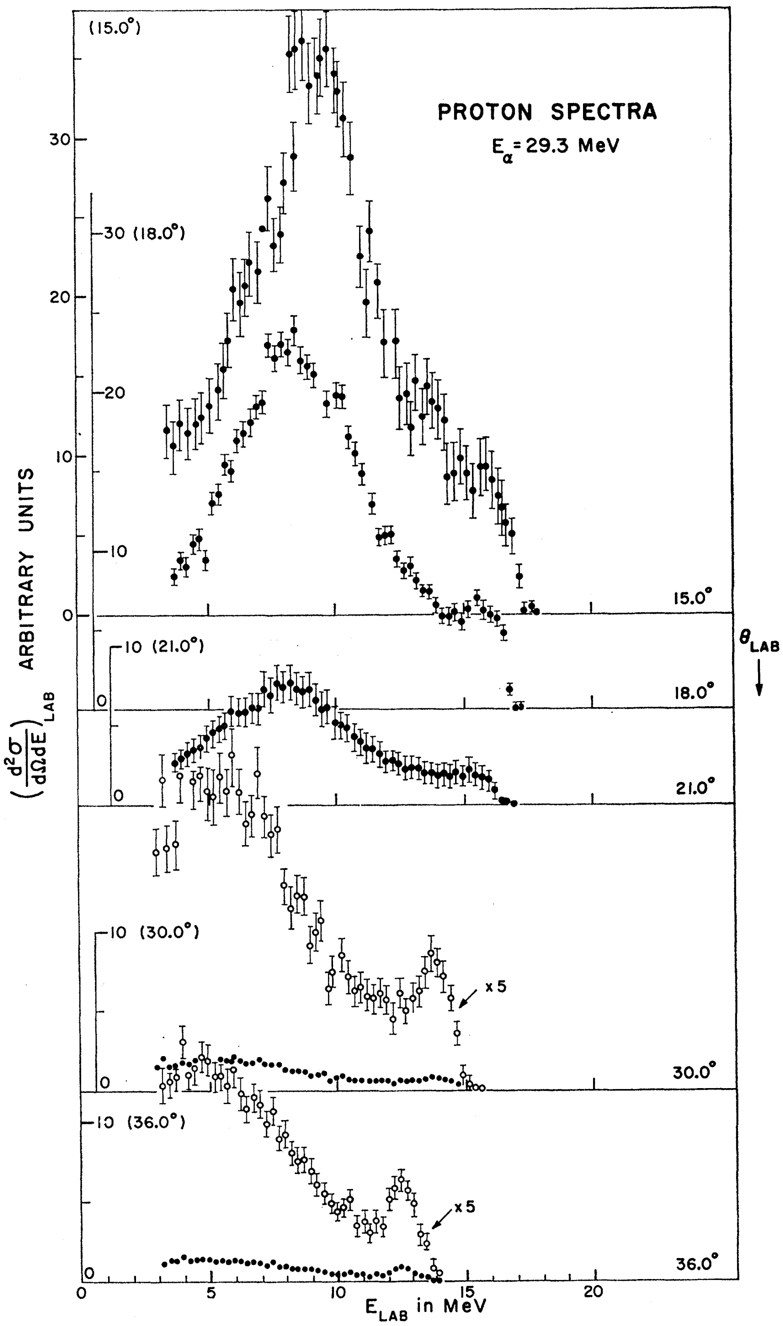


FIG. 6. Proton spectra as in Fig. 3 but at a reduced incident alpha-particle energy of 29.3 MeV.

prediction, in the center-of-mass system, bears essentially no resemblance to the experimental data, as anticipated.

Turning then to the Born-approximation calculation we make use of the $t$-matrix formalism and the Lippmann-Schwinger integral equation.[28]

The matrix element $M$ in this approximation may be expressed as

$$M=\langle\Phi_f|t|\Phi_i\rangle\,, \tag{4}$$

where the initial and final wave functions are given by

$$\Phi_i\propto(e^{i\mathbf{K}_{\alpha_i}\cdot\mathbf{r}_\alpha})(e^{i\mathbf{K}_d\cdot\mathbf{r}_d})\Phi_d(\mathbf{r}_n-\mathbf{r}_p)\,, \tag{5}$$

$$\Phi_f\propto(e^{i\mathbf{K}_{\alpha_f}\cdot\mathbf{r}_\alpha})(e^{i\mathbf{K}_n\cdot\mathbf{r}_n})(e^{i\mathbf{K}_p\cdot\mathbf{r}_p})\,, \tag{6}$$

where in Eq. (5) $\Phi_d(\mathbf{r}_n-\mathbf{r}_p)$ represents the deuteron internal wave function. The Hamiltonians in the

[28] We are particularly indebted to Professor K. R. Greider for numerous discussions concerning this formalism.

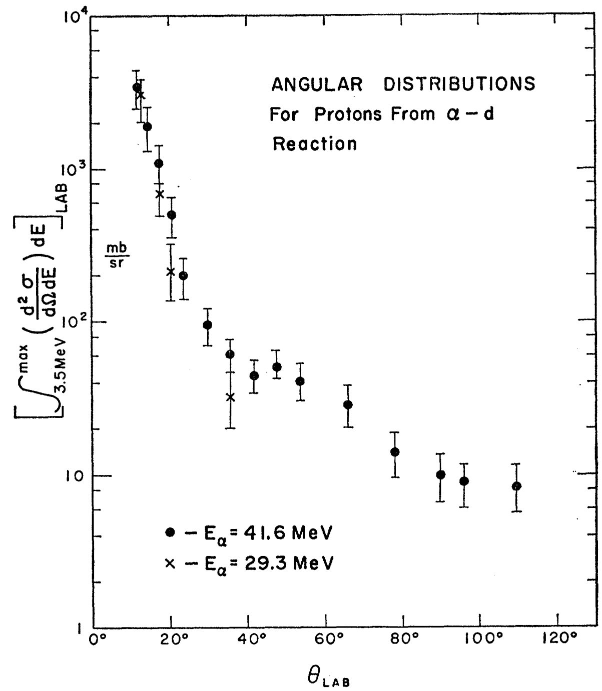


FIG. 7. Proton angular distribution from alpha-particle-induced deuteron dissociation. In obtaining this distribution all protons at energies in excess of 3.5 MeV have been included. The relevant alpha-particle energies are indicated in the figure.

asymptotic initial and final states may be written as

$$H_i = T + V_{np}, \tag{7}$$

$$H_f = T, \tag{8}$$

with

$$T = T_\alpha + T_n + T_p. \tag{9}$$

The wave functions are correspondingly defined as

$$(H_i - E)\Phi_i = 0, \tag{10}$$

$$(H_f - E)\Phi_f = 0, \tag{11}$$

and the complete system Hamiltonian is given by

$$H = T + V_{np} + V_{\alpha n} + V_{\alpha p}. \tag{12}$$

Using the Lippmann-Schwinger equation, the complete wave function asymptotic to $\Phi_i$ may be written as

$$|\Psi_i^{(+)}\rangle = [1 + (E - H + i\epsilon)^{-1}(V_{\alpha n} + V_{\alpha p})]|\Phi_i\rangle. \tag{13}$$

Similarly, the complete wave function asymptotic to $\Phi_f$ is written as

$$|\Psi_f^{(-)}\rangle = [1 + (V_{np} + V_{\alpha n} + V_{\alpha p})(E - H - i\epsilon)^{-1}]|\Phi_f\rangle. \tag{14}$$

The matrix element $M$ is, by definition,

$$\begin{aligned} M &= \langle \Psi_f^{(-)} | V_{\alpha n} + V_{\alpha p} | \Phi_i \rangle \\ &= \langle \Phi_f | t | \Phi \rangle, \end{aligned} \tag{15}$$

where

$$t = [1 + (V_{np} + V_{\alpha n} + V_{\alpha p})(E - H - i\epsilon)^{-1}](V_{\alpha n} + V_{\alpha p}). \tag{16}$$

In Born approximation only the first term of Eq. (16) is taken into account:

$$t^B = V_{\alpha n} + V_{\alpha p}, \tag{17}$$

$$M^B = \langle \Phi_f | V_{\alpha n} + V_{\alpha p} | \Phi_i \rangle. \tag{18}$$

To keep the computations tractable several approximations have been made. Only relative $S$ states in the deuteron have been considered and all effects of tensor forces have been ignored. The asymptotic form of the Hulthén deuteron wave function has been used; i.e.,

$$\Phi_d(r_{np}) \propto e^{-\alpha r_{np}}/r_{np} \tag{19}$$

where $r_{np} = |\mathbf{r}_n - \mathbf{r}_p|$ and $\alpha = (-MQ/\hbar^2)^{1/2}$, where $Q$ is the deuteron binding energy. The Born-approximation matrix element corresponding to Eq. (18) may then be written as

$$\begin{aligned} M^B = &\left[\int e^{i\mathbf{q}_\alpha \cdot \mathbf{r}_{\alpha p}} V_{\alpha p} d^3 r_{\alpha p}\right] \int e^{i\mathbf{q}_n \cdot \mathbf{r}_{np}} \frac{e^{-\alpha r_{np}}}{r_{np}} d^3 r_{np} \\ &+ \left[\int e^{i\mathbf{q}_\alpha \cdot \mathbf{r}_{\alpha n}} V_{\alpha n} d^3 r_{\alpha n}\right] \int e^{i\mathbf{q}_p \cdot \mathbf{r}_{pn}} \frac{e^{-dr_{pn}}}{r_{pn}} d^3 r_{pn}, \end{aligned} \tag{20}$$

where $\mathbf{q}_j$ represents the momentum transfer defined as

$$\begin{aligned} \mathbf{q}_\alpha &\equiv \mathbf{K}_{\alpha_i} - \mathbf{K}_{\alpha_f}, \\ \mathbf{q}_p &\equiv \tfrac{1}{2}\mathbf{K}_d - \mathbf{K}_p, \\ \mathbf{q}_n &\equiv \tfrac{1}{2}\mathbf{K}_d - \mathbf{K}_n, \end{aligned} \tag{21}$$

and the relative coordinate position vector $\mathbf{r}_{ij}$ is given by

$$\begin{aligned} \mathbf{r}_{\alpha p} &\equiv \mathbf{r}_\alpha - \mathbf{r}_p, \\ \mathbf{r}_{\alpha n} &\equiv \mathbf{r}_\alpha - \mathbf{r}_n. \end{aligned} \tag{22}$$

A further simplification has been made in that $V_{\alpha p}$ and $V_{\alpha n}$ appearing in Eq. (20) have been replaced with zero-range potentials. Under these conditions the matrix element takes the form

$$M^B = \text{constant} \times [(q_n^2 + \alpha^2)^{-1} + (q_p^2 + \alpha^2)^{-1}] \tag{23}$$

and the corresponding spectrum prediction is shown as curve 3 of Fig. 10. It should be noted that in the cross section there are contributions from both the $q_n$ and $q_p$ terms in Eq. (23) in addition to an interference contribution. The major part of the predicted yield at high energies comes from the $q_n$ term and at low energies from the $q_p$ term; the interference term contributes at all energies.

Again, it is obvious that the zero-range Born approximation does not suffice to reproduce any of the structure in the experimental spectrum. This is of course anticipated since this approximation does not include any resonant character in the alpha-neutron interactions.

In an attempt to introduce these resonances in more

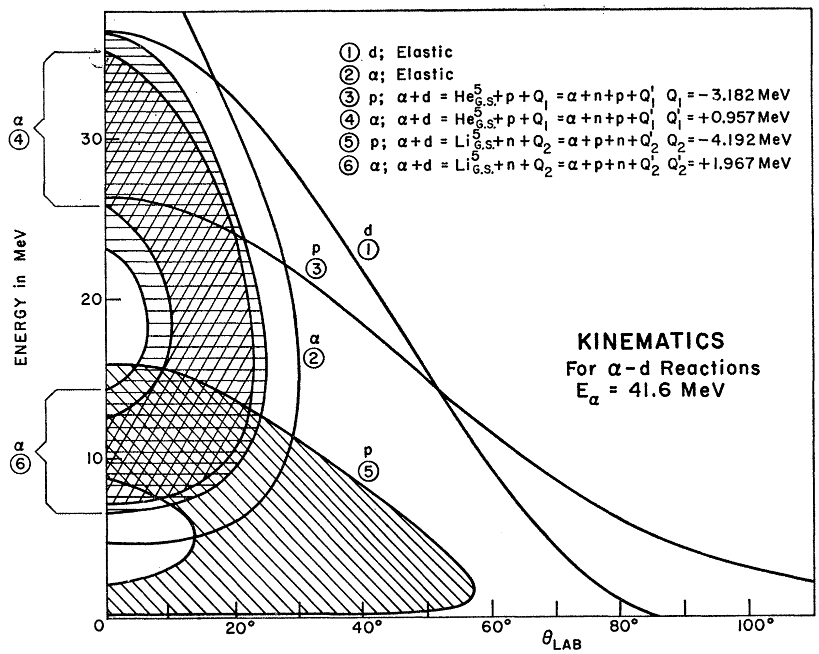


FIG. 8. Kinematic plots for the alpha-particle-induced dissociation of the deuteron at an incident energy of 41.6 MeV. The relevant particles and production mechanisms are indicated in the legend of the figure (G.S.≡ground state).

explicit fashion the $t$ matrix may be approximated as

$$t \approx t_{\alpha n} + t_{\alpha p}\,, \tag{24}$$

where

$$t_{\alpha n} \equiv [1 + V_{\alpha n}(E - T - V_{\alpha n} + i\epsilon)^{-1}]V_{\alpha n}\,, \tag{25}$$

$$t_{\alpha p} \equiv [1 + V_{\alpha p}(E - T - V_{\alpha p} + i\epsilon)^{-1}]V_{\alpha p}\,. \tag{26}$$

In this approximation, the transition matrix element is then written as

$$M \approx \langle \Phi_f | t_{\alpha n} | \Phi_i \rangle + \langle \Phi_f | t_{\alpha p} | \Phi_i \rangle\,, \tag{27}$$

where it is noted that $t_{\alpha n}$ and $t_{\alpha p}$ are the two-body $t$ matrices for free $\alpha$-$n$ and $\alpha$-$p$ scattering and $M$ given by Eq. (27) illustrates a quasifree process. In effect, we are here retaining several additional terms in Eq. (16) beyond those of the Born approximation. For reasons given above the details of the cross-section calculation using the matrix element of Eq. (27) will only be summarized herein and reported in greater detail in a later publication.[29]

It should be noted that in Eqs. (16), (25), and (26) the neutron and proton interaction in the final state has been completely neglected. This may be justified by the fact that after the scattering due to $V_{\alpha n}$ (or $V_{\alpha p}$)

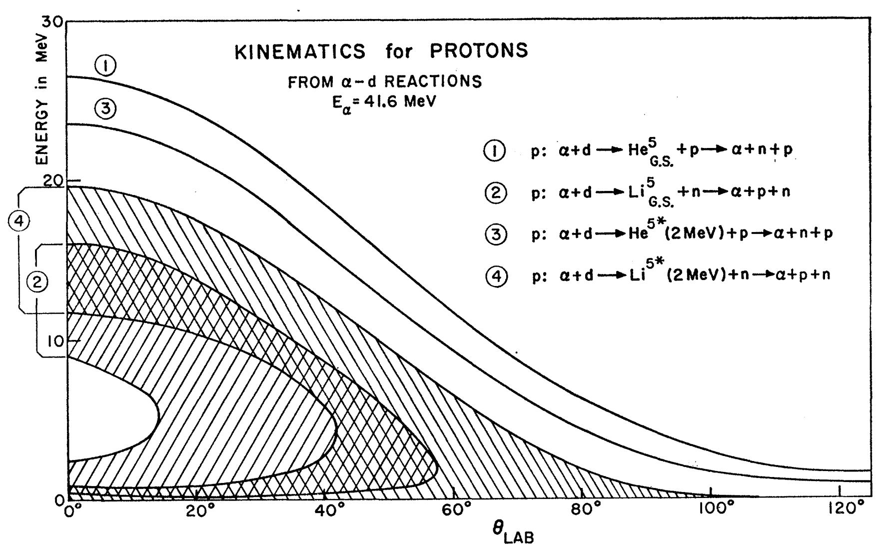


FIG. 9. Kinematic plot for protons from the alpha-particle-induced dissociation of the deuteron at an incident energy of 41.6 MeV. The relevant particles and production mechanisms are indicated in the legend of the figure.

[29] H. Nakamura, K. Nagatani, and D. A. Bromley (to be published).

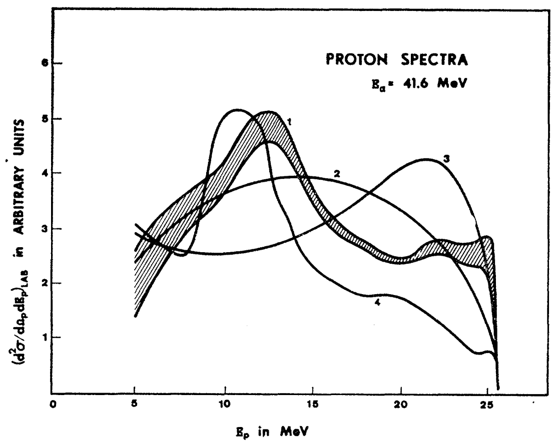


FIG. 10. Predicted and experimental proton energy spectra. The broad curve 1 represents the experimental data. The upper bound of the hatched region gives the result before correction for spectrum tail effects as discussed in the text; the lower bound marks an upper bound to the magnitude of this effect, hence a lower bound to the experimental data after correction. Curve 2 is the phase-space prediction and curve 3 corresponds to the zero-range Born approximation calculation. Curve 4 is the prediction based on use of the Gammel-Thaler potentials to represent the resonant final-state interactions. All curves are arbitrarily normalized to the same area above 5 MeV to facilitate presentation here.

the neutron and proton have low probability of being found within their mutual interaction range for scattering in continuum states. Consequently, the interaction $V_{np}$ in the final state is expected to be unimportant *unless* a resonance occurs in the interaction. However, it is known that the only $n$-$p$ resonance which occurs is one in a $T=1$ state which cannot be realized in this reaction to the extent that isobaric spin conservation holds.

Furthermore, in the $t$ matrix of Eqs. (25) and (26) the interaction between the alpha particle and both the neutron and proton has been neglected. This neglect is based on the argument that the alpha particle and deuteron have widely different binding energies and that in consequence it is realistic to consider the dissociation as proceeding through an effective quasifree scattering of the alpha particle from either the neutron or proton. The success obtained in the present calculations indeed provides *a posteriori* justification for such an assumption although this effect should be included in a more complete analysis.

In the actual calculations the $V_{\alpha n}$ and $V_{\alpha p}$ appearing in Eqs. (25) and (26) have been taken as represented by the phenomenological Gammel-Thaler potentials[30] derived to describe free alpha-nucleon scattering. We are thus assuming that these potentials will provide an adequate representation of the matrix elements off the energy shell. All Coulomb forces have been neglected and the partial waves appearing in the expansions of $t_{\alpha n}$ and $t_{\alpha p}$ have been terminated at $p_{3/2}$. The predicted spectrum is shown as curve 4 of Fig. 10. It should be noted that the highest energy peak appearing in the experiment is reproduced by the calculations where it is found to reflect the $p_{3/2}$ resonance in the alpha-neutron interaction. The peak at about 10 MeV in the calculated spectrum reflects the presence of a $p_{3/2}$ resonance in the alpha-proton interaction. The fact that it appears at lower energy than the corresponding peak in the experimental spectrum almost certainly reflects the neglect of Coulomb effects in the calculations. Inclusion of such effects would necessarily shift the calculated proton peak to higher proton energies.

The calculated absolute cross section at this angle for proton energies above 5 MeV is approximately 1.2 mb/sr while the experimental value obtained is $3.3\pm1.2$ mb/sr.

## V. CONCLUSIONS

Striking evidence for resonant final-state interactions has been obtained in the alpha-particle-induced dissociation of the deuteron. The experimental proton-energy spectrum and absolute cross section have been adequately fitted by an approximate calculation which explicitly includes the alpha-nucleon resonances represented by phenomenological Gammel-Thaler potentials. The success thus far attained in the approximate calculations justifies a much less approximate calculation where it might be hoped that the experimental data might be used to elucidate details of the deuteron wave function and of the alpha-nucleon scattering matrix elements off the energy shell. Much more extensive particle-particle coincidence data would be extremely useful in testing such calculations and in providing new input concerning the details of the dissociation mechanism.

## ACKNOWLEDGMENTS

The authors are indebted to Professor K. R. Greider for extensive discussions, to Dr. H. Nakamura for collaboration in the $t$-matrix calculations, and to Dr. Č. Zupančič and Dr. P. F. Donovan for information concerning their measurement prior to its publication. Professor J. C. Overley, J. Birnbaum, and J. E. Poth assisted in taking some of the experimental data.

[30] J. L. Gammel and R. M. Thaler, Phys. Rev. **109**, 2041 (1958).